Journal of Fluids and Structures 17 (2003) 783–791

JOURNAL OF FLUIDS AND STRUCTURES

www.elsevier.nl/locate/jnlabr/yjfls

Flow around a circular cylinder downstream of a blunt-based flat plate in tandem and staggered arrangements

H.İ. Keser, M.F. Ünal*

Faculty of Aeronautics and Astronautics, Istanbul Technical University 80626 Maslak-Istanbul, Turkey

Received 17 July 2001; accepted 14 January 2003

Abstract

Using an experimental approach, flow around a blunt-based flat plate of thickness H and a downstream circular cylinder of diameter $D=0.75H$ in tandem and staggered arrangements have been investigated at Reynolds numbers of $Re_\ell = 1.46\times10^5$, 2.72×10^5 and 3.71×10^5 based on the plate length ℓ. The investigation focuses on the effect of a wide range of values of longitudinal and transverse spacing between the plate and the cylinder on the mean pressure distributions around the base of the plate and the cylinder as well as the drag and lift coefficients of the cylinder. For both the tandem and the staggered arrangements the mean pressure distributions indicate the existence of a critical spacing on either side of which different flow interferences take place.
© 2003 Elsevier Science Ltd. All rights reserved.

1. Introduction

Interfering wakes of two bluff bodies placed in a uniform flow lead to vortex shedding and aerodynamic characteristics that are drastically different from those found in the case of a single body. Considerable insight into variations of these characteristics depending on the arrangements of bodies has been provided mainly by experimental studies. Extensive review articles by Zdravkovich (1977, 1987) summarize important research contributions and recent studies of Sumner et al. (2000) and Gu and Sun (1999) provide more insight into the interference between circular cylinders of the same diameter, which, among various body shapes, has received most research attention.

However, relatively little has been done for the case of bluff bodies of different cross-stream length scales. According to an experimental study of tandem circular cylinders of different diameters ($D_2/D_1=0.68$; D_2 and D_1 are diameters of downstream and upstream cylinders respectively), for small spacing (i.e. $L/D_1\leqslant1$; L is the distance between centers of the cylinders), the separated layers from the upstream cylinder do not reattach onto the downstream one (Igarashi, 1982). However, as the spacing increases, different flow patterns extending from reattachment in synchronization with vortex shedding from the downstream cylinder to quasi-steady vortex formation in front of the cylinder are observed. Further increase to a critical spacing results in roll-up of separated boundary layers in front of the cylinder. The appearance of these flow patterns depends not only on the spacing but also on Reynolds number (Okajima, 1979) and the diameter ratio of two cylinders (Hiwada et al., 1979).

To the authors' knowledge, wake of a long blunt-end plate interacting with a downstream bluff body has not been reported before. This case differs from that of circular cylinders, in that, the boundary layers developing on upper and lower surfaces of the plate become relatively thicker before they reach to the blunt-end. Consequently, the flow patterns described above for the cylinders are expected to modify accordingly. The primary objective of the present study is to

*Corresponding author.
E-mail addresses: keser@itu.edu.tr (H.İ. Keser), munal@itu.edu.tr (M.F. Ünal).

0889-9746/03/$ - see front matter © 2003 Elsevier Science Ltd. All rights reserved.
doi:10.1016/S0889-9746(03)00022-7

Nomenclature

C_D	drag coefficient
C_L	lift coefficient
C_p	pressure coefficient
C_{PG}	pressure coefficient at front stagnation of cylinder
C_{PS1}	pressure coefficient at back stagnation point of plate
C_{PS2}	pressure coefficient at back stagnation of cylinder
D	diameter of cylinder
E	transverse spacing between bodies
H	plate trailing end thickness
L	longitudinal spacing between bodies
ℓ	chord length of plate
Re_ℓ	Reynolds number based on the plate length
p_o	free stream pressure
p	pressure
s	distance along surface
U_o	uniform velocity
θ	angle from the front stagnation point of the cylinder
ρ_o	free stream density

disclose these modifications in terms of experimentally found mean pressure distributions around a circular cylinder placed downstream of a blunt-based flat plate in tandem and staggered arrangements (Fig. 1).

2. Experimental arrangement

Experimental investigation has been carried out using an open-circuit wind tunnel at the Reynolds numbers based on the plate length (ℓ), $\mathrm{Re}_\ell = 1.46 \times 10^5$, 2.72×10^5 and 3.71×10^5 (Keser, 1995). The maximum turbulence level of the tunnel in this Reynolds number range is 0.2%. The test-section is 50 cm high and 50 cm wide. In order to eliminate the unfavorable effects of the boundary layers developing on walls of the wind tunnel, a Plexiglas insert test-section is used. This test-section is 40 cm wide, 38 cm high and 170 cm long. $H = 4$ cm thick and $\ell = 52.7$ cm long flat plate with a rectangular trailing-end is rigidly placed into the insert test-section. At the mid span of the plate, the trailing-end has 10 equidistant pressure taps on both upper and lower faces and 5 taps on the back face. With a minimum distance of 10 mm from the trailing edge, the pressure taps on the upper and lower surfaces have constant spacing of 10 mm. At the base, uppermost and lowermost taps are 10 mm away from the corners and the distance between the consecutive taps is 5 mm. In order to prevent separation of flow, the leading edge of this plate is chosen to be a semi-ellipse, length ratio of whose axes is 5:1. Smoke visualization showed smooth, un-separated flow on upper and lower sides of the plate. The circular cylinder placed directly downstream is made from an aluminum tube having an outer diameter of $D = 3$ cm and a wall thickness of 6 mm. The cylinder is divided into three sections. The middle section, which is 7.6 cm long, contains eight pressure taps around its circumference with equal intervals. This section, when smoothly joined with the two side

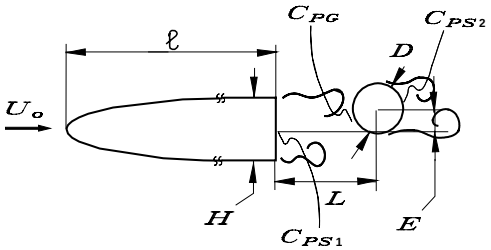

Fig. 1. Flow configuration and various parameters of the study.

sections spans the width of the insert test-section. By turning the cylinder around its axis, pressure measurements have been taken at a total of 32 points. All the pressure taps are 10 mm deep and have 0.8 mm bore. Measurements of mean pressure distributions are taken by connecting the pressure taps directly to an electro-pneumatic micromanometer (FURNESS FC001). The connecting plastic tubes have inner diameters of 1 mm and lengths of 60 cm. Mean pressure measurements for the above-mentioned Reynolds numbers are done at a maximum of 12 different longitudinal spacing, namely, $L/H=0.65$, 1, 1.5, 2, 2.5, 2.85, 3, 4, 5, 6, 8 and 10 at four different transverse spacing values $E/H=0$, 0.25, 0.5, 1 (Fig. 1). The pressure coefficient is defined as $C_p=(p-p_o)/0.5\rho_o U_o^2$, where the pressure, density and velocity of the oncoming flow are denoted by p_o, ρ_o and U_o, respectively.

For the transverse spacing $E/H=0$ symmetric mean pressure distributions around both the base of the plate and the downstream circular cylinder with respect to the centerline provided a check on the alignment of the plate and the cylinder with the flow. Additionally, dynamic pressure measurements by means of a Pitot-static tube along the width of the wind tunnel in the approaching flow to the plate assured that the flow is uniform within at least the central 80% of the span. To minimize the errors in the pressure measurements, special care was taken to open the pressure taps in the direction of the local surface normal and without burrs. The length-to-diameter ratio of the pressure taps was made as small as possible. During the experiments, the atmospheric pressure experiences a small variation between 760–761.7 mmHg. The manometer has an accuracy of ± 0.1 mm of water. On the other hand, error due to the reading by eye is estimated to be at the order of 2%. For the square-edged pressure holes having 0.8 mm hole size, the percentage error in the dynamic head ($\rho_o U_o^2/2=36.6\,\mathrm{N/m^2}$ for $\mathrm{Re}_\ell=2.72\times10^5$) is 0.32% (Breugelmans and Junkhan, 1973), which amounts to an error much smaller than the error of the measurement device, i.e. 0.02 mm H_2O. The errors in the vicinity of the front stagnation point on the cylinder are expected to be large. However, repeatability of the measurements has been extensively checked, and it has been found that the measurements are repeatable to within $\pm 1.5\%$ accuracy.

3. Discussion of results

3.1. Tandem arrangement

The measured mean pressure coefficient distributions (Fig. 2) as function of θ (angle from the front stagnation point in clockwise direction) for a total of 12 different longitudinal spacing (L/H) in tandem arrangement of the plate and the cylinder for $\mathrm{Re}_\ell=2.72\times10^5$ and $D/H=0.75$ lead to classification of flow patterns depending on (L/H). The variations of the pressure distributions around the cylinder with L/H described below are also valid for the other Reynolds numbers of the study, namely $\mathrm{Re}_\ell=1.46\times10^5$ and 3.71×10^5, and thus are not presented here.

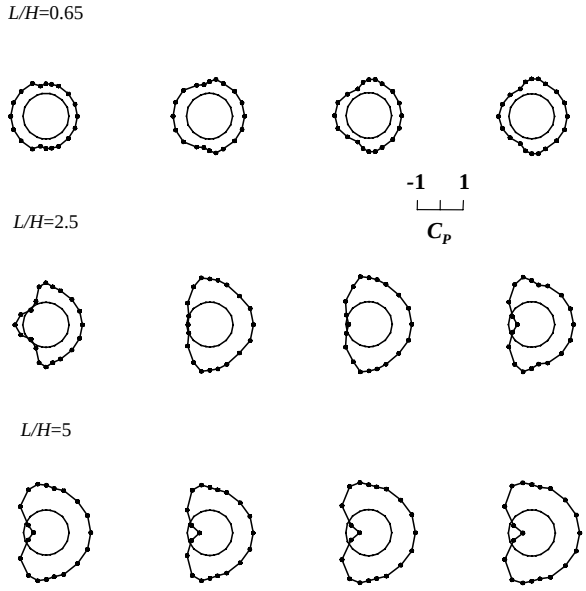

Fig. 2. Mean pressure coefficient (C_P) distributions on the cylinder surface for $L/H=0.65$, 1, 1.5, 2, 2.5, 2.85, 3, 4, 5, 6, 8 and 10 (from left to right, from top to bottom) at $\mathrm{Re}_\ell=2.72\times10^5$.

Within the range of $0.65 \leqslant L/H \leqslant 2.5$, the C_P versus θ distributions have suction minima at angles other than $\theta = 0^\circ$ (Fig. 2), which indicate symmetric boundary layer reattachment of the separated layers from the plate onto the cylinder surface there. For $L/H = 1.5$ and 2, suction minima are evident at $\theta \cong \pm 65^\circ$. As the spacing increases from $L/H = 2$ to 2.5, these minima become pronounced and move towards the front stagnation point. For $L/H = 1$, 1.5, 2 and 2.5, there are also suction maxima around the shoulders of the cylinder, indicating flow separation from there.

Common to all $L/H \leqslant 2.5$ is the fact that, the pressure coefficient at the front stagnation of the cylinder (C_{PG}) is approximately equal or slightly larger than that at the stagnation point of the plate (C_{PS1}), which indicates a stagnant flow in the gap between the plate and the cylinder [Fig. 3(a)]. The stagnant gap flow is presumably caused by the delay of evolution of the separated boundary layers into vortices by the presence of the downstream cylinder.

For the smallest spacing $L/H = 0.65$, suction in front of the cylinder (C_{PG}) is larger with respect to that at the back (C_{PS2}), whereas for $L/H = 1$, these two suction values are almost equal [Fig. 3(b)]. From $L/H = 0.65$ to 2.5, the negative pressure coefficient at the base of the cylinder (C_{PS2}), similar to those at the shoulders, steadily increases with respect to the gap pressure (C_{PG}), which indicates enhancement of vortex formation activity with increasing L/H behind the cylinder [Fig. 3(b)]. Corresponding to the increase of the suction C_{PS2} with L/H, both of the suction values at the stagnation point of the plate (C_{PS1}) and that at the front stagnation point of the cylinder (C_{PG}) follow the reverse trend and decrease. However their ratio remains close to unity [Figs. 2 and 3(a)].

Passing from $L/H = 2.5$ to 2.85, there is a drastic variation of the pressure distribution: The suction minimum for $L/H = 2.85$ is now at $\theta = 0^\circ$, and unlike the cases for $L/H \leqslant 2.5$, there is a large difference between the C_{PG} and C_{PS1} [Figs. 2 and 3(a)]. The sudden decrease of the C_{PG}/C_{PS1} ratio is primarily due to a sudden increase of C_{PG} to a small positive value, rather than a decrease in the value of C_{PS1} which is always negative. Evidently, at that spacing, the vortex formation from the plate is taking place in front of the cylinder and interacting with it, i.e. a "jump" of flow is experienced as reported before for equal and unequal diameter cylinder pairs in tandem arrangements by Igarashi (1981, 1982).

For the case of cylinders of equal diameters, reported values of the critical spacing marking the beginning of the jumped flow, i.e. the beginning of the region in which the maximum pressure coefficient is at $\theta = 0^\circ$, varies between 3.5 and 3.8 diameters, whereas for circular cylinders with a diameter ratio of upstream to downstream cylinder $D_2/D_1 = 0.68$, the critical spacing varies between 2 and 2.6 diameter of the upstream cylinder, at higher and lower Reynolds numbers respectively. The critical spacing $L/H = 2.85$ of this study is close to the previously reported value of 2.6 (Igarashi, 1982).

However, the variations of C_{PS1}, C_{PG} and C_{PS2} described above are substantially different from those previously put forward for circular cylinders of unequal diameters by Igarashi (1982): For $D_1/D_2 = 0.68$ at $\mathrm{Re}_{D1} = 3.2 \times 10^4$, before the jump in the flow pattern occurs, there are three different flow patterns depending on the longitudinal spacing. The first flow pattern is a "complete separation" type for sufficiently small spacing in which the separated layers from the upstream cylinder do not reattach onto the downstream one. On the contrary, as demonstrated above, suction minima indicating reattachment are evident for the plate-cylinder configuration even for the smallest spacing of $L/H = 0.65$ (Fig. 2). The second and third patterns put forward by Igarashi (1982) are reattachment flows in which the shear layers reattach onto the second cylinder. In the second pattern, the flow around the downstream cylinder becomes regular, because the attachment on the rear surface of the cylinder of the shed vortices from one side of the upstream cylinder is accompanied by "synchronized reattachment" of the other separated layer from the upstream onto the front surface of the downstream cylinder. Consequently, the gap pressure coefficient between the two cylinders decreases remarkably and the drag coefficient of the downstream cylinder acts as a large thrust, i.e. the cylinder is drawn towards upstream. The third pattern is characterized by formation of quasi-steady reattachment of shear layers from the upstream cylinder

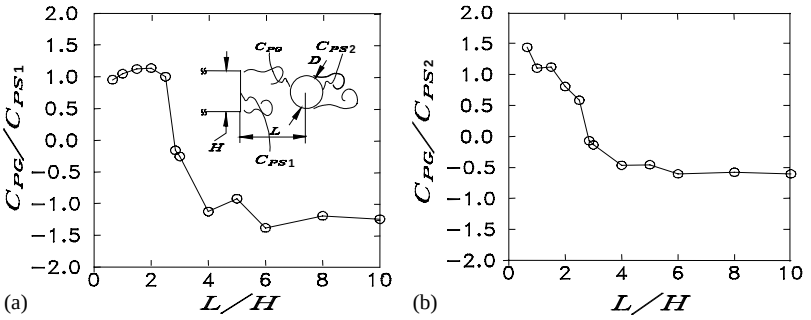

Fig. 3. Variation of C_{PG}/C_{PS1} (a) and C_{PG}/C_{PS2} (b) with respect to L/H at $\mathrm{Re}_\ell = 2.72 \times 10^5$.

to the downstream one. As opposed to those three different flow patterns, the only flow pattern implied by the mean pressure distributions on the cylinder and variations with respect to L/H of C_{PS1}, C_{PG} and C_{PS2}, before the critical longitudinal spacing of this study is the quasi-steady reattachment flow pattern. At the beginning of the interval $0.65 \leqslant L/H \leqslant 2.5$ in which the ratio of C_{PG}/C_{PS1} is almost unity, the drag coefficient of the cylinder is slightly negative (Fig. 4). Within the range of $1.5 \leqslant L/H \leqslant 2.5$, where the reattachment points of the boundary layers move upstream with increasing L/H (Fig. 2), the drag coefficient of the downstream cylinder continuously increases. For spacings larger than the critical $L/H = 2.85$, as L/H increases the drag coefficient C_D continues to increase with a smaller rate in comparison with that for $L/H \leqslant 2.5$.

In summary, the variations with L/H of C_{PS1}, C_{PG} and C_{PS2} up to $L/H = 2.5$ makes it evident that, up to the critical distance there is a single flow pattern encountered in this study. Presumably, due to the fact that the boundary layers on the upper and lower surfaces of the plate develop into much thicker separated layers and the cross-stream length scale ratio is larger in comparison with the case of a cylinder pair of unequal diameters (Igarashi, 1982), the above-described "complete reattachment" and "synchronized flow" patterns are by-passed and thus the gap flow remained stagnant for large values of spacing, extending up to the critical.

3.2. Staggered arrangement

The critical longitudinal spacing of the tandem arrangement is similarly important for all the staggered arrangements of the study. In contrast to those for larger longitudinal spacings, for $L/H \leqslant 2$, the pressure distributions around the trailing-end of the plate for all values of the transverse spacing extending from $E/H = 0.25$ to 1.0 are clearly asymmetric (Fig. 5). However, for $L/H \geqslant 3$, the pressure distributions for all E/H become similar to the symmetrical distributions of $E/H = 0$, except that the base pressure variation from one L/H to another is more pronounced for $E/H = 0$ (Fig. 5). It follows that, a critical longitudinal spacing of similar value to that of the tandem arrangement, i.e. $L/H = 2.5$–3.0, marks the beginning of the region in which the wake of the plate is relatively less influenced by the presence of the downstream cylinder for all the staggered arrangements of this study.

With respect to the corresponding values of the tandem arrangement, the values of base suction for L/H=1 and 2 increase from E/H=0.25 onward especially for L/H=1 and imply a deflected gap flow between the plate and the cylinder. In agreement with that is the higher degree of blockage effect of the downstream cylinder for increasing E/H, which is evidenced by smaller suction values on the upper surface of the plate, and the higher suction values corresponding to increased flow rate on the lower surface with respect to the tandem arrangement.

On the other hand, the most obvious difference in the mean pressure distributions on the cylinder surface in comparison with the case of tandem arrangement (Fig. 6) is that the maximum pressure coefficient location on the cylinder is not coincident with $\theta = 0^{\circ}$, but is shifted towards outside of the gap. The shift in the location of the pressure coefficient of unity indicates an oncoming mean flow deflection towards the gap. The amount of deflection depends on both the longitudinal L/H and transverse E/H spacings between the plate and the cylinder and is larger for smaller E/H. For a constant E/H, the deflection decreases with increasing L/H.

In conformity with the implied deflected mean flow towards the gap between the bodies, the maximum pressure coefficient remains constant at around unity for all the staggered arrangements E/H=0.25, 0.5 and 1 when $L/H < 3$. For E/H=0.25, the pressure distributions at L/H=1 and 2 are similar to the pattern $\mathrm{II_B}$ described by Gu and Sun (1999) for a

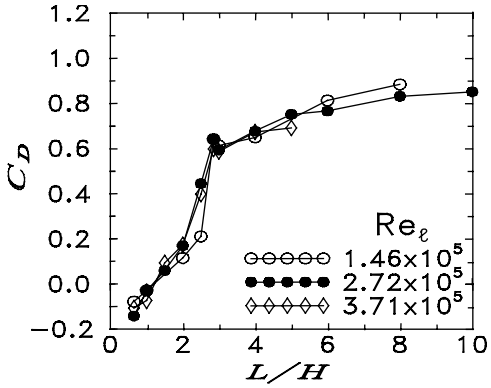

Fig. 4. Variation of drag coefficient (C_D) with respect to L/H.

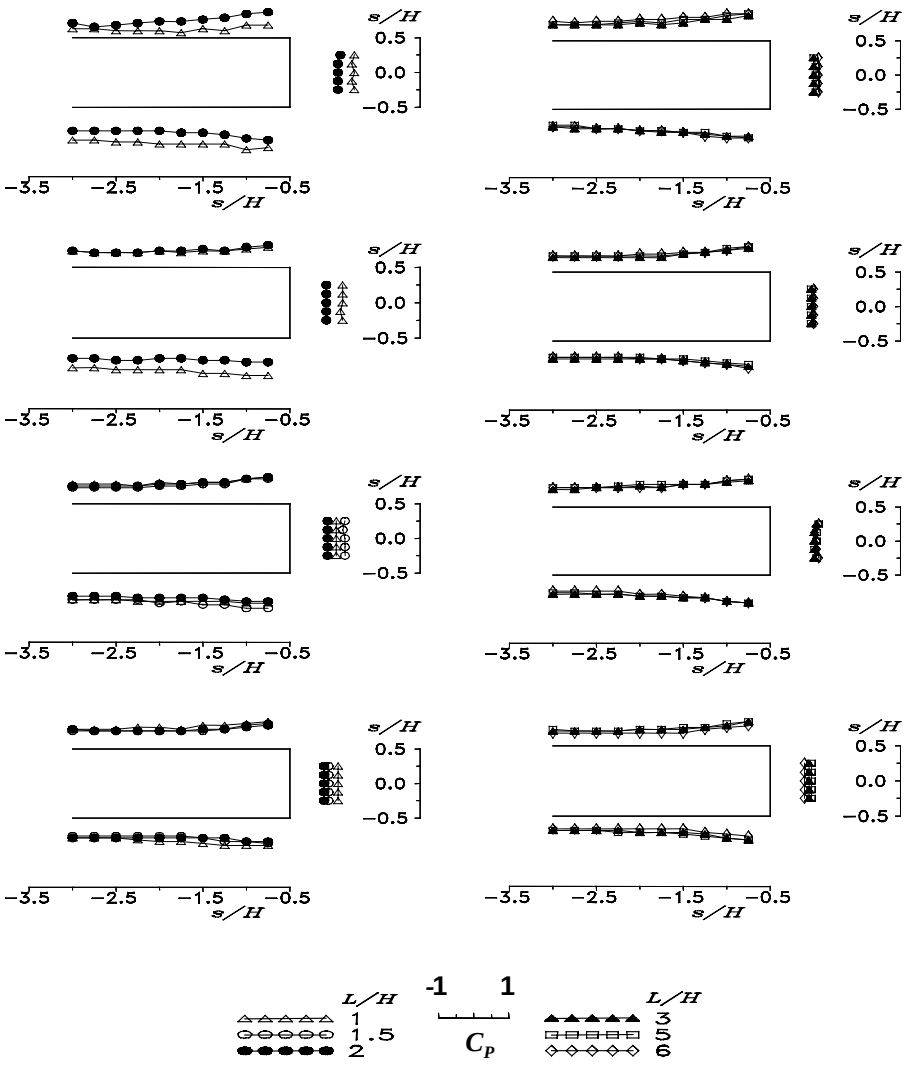

Fig. 5. Distributions of the mean pressure coefficient (C_P) on surfaces of the trailing-end of the plate as function of longitudinal separation (L/H) for $E/H=0.0$, 0.25, 0.5, 1.0 (from bottom to top) at $\mathrm{Re}_\ell = 2.72\times10^5$.

pair of staggered cylinders of equal diameters in the high subcritical regime. Pattern $\mathrm{II_B}$ is characterized by a large, strong suction area on the gap-side of the downstream cylinder: As pointed out by Gu and Sun (1999), due to the fact that the separated shear layer from the gap-side of the upstream body reattaches with its high speed side onto and separates again from the gap-side surface of the downstream cylinder, the suction values on a large portion of the cylinder surface facing the upstream plate and its wake are higher (Fig. 6). This pattern is consistent with the induced separation flow pattern of Sumner et al. (2000), the inner shear layer from the upstream cylinder is deflected into the gap between the cylinders.

As E/H increases to 0.5 and 1.0 for $L/H<3$, both the angle of stagnation point with respect to horizontal and the suction on the gap-side of the cylinder gradually reduces. The pressure distributions for E/H=1.0 resemble the pattern $\mathrm{III_B}$ on the downstream cylinder encountered for similar values of transverse and longitudinal spacing in the case of circular cylinder pair of equal diameters (Gu and Sun, 1999). The pattern $\mathrm{III_B}$ is characterized with the disappearance of the pronounced suction on the gap-side surface of the cylinder. The corresponding flow structure between the cylinders is depicted as the one in which, unlike the case for $E/H=0.25$ and $L/H<3$, the separated layers from the gap-side of the upstream body no longer reattach onto the downstream cylinder, but individual wake regions of the upstream and downstream bodies as well as the oncoming mean flow penetrating the gap between the bodies are established (Gu and Sun, 1999; Sumner et al., 2000).

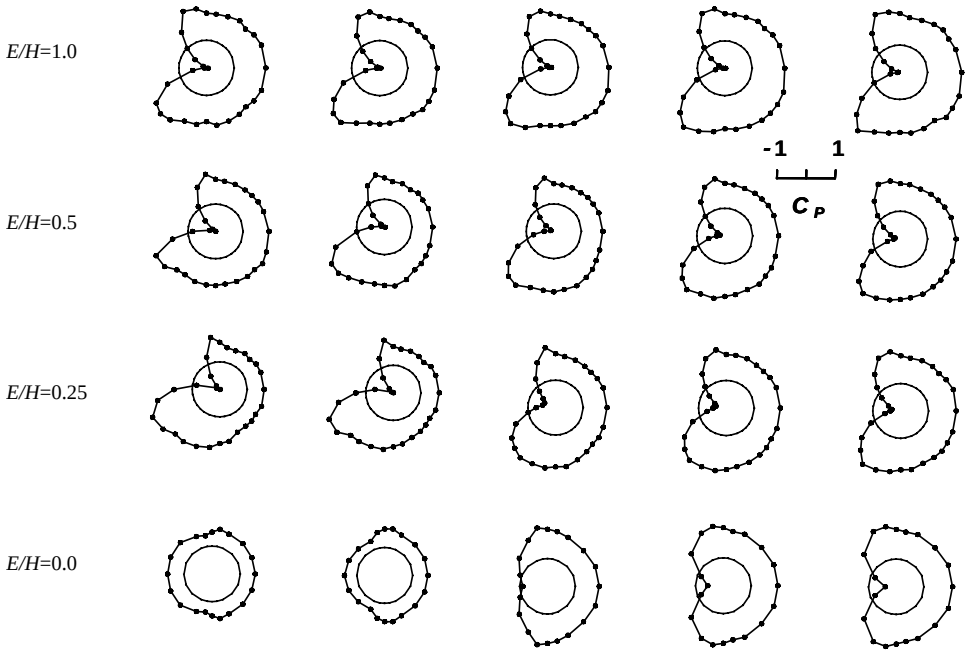

Fig. 6. Mean pressure coefficient distributions around the cylinder for $L/H = 1, 2, 3, 5, 8$ (from left to right) and $E/H = 0.0, 0.25, 0.5, 1.0$ (from bottom to top).

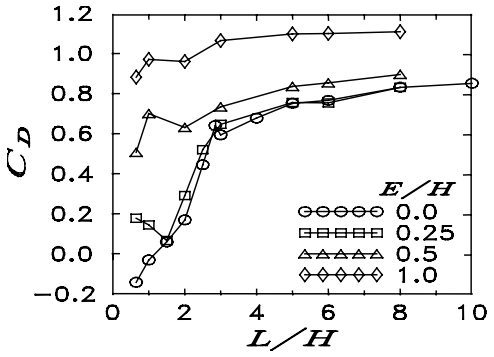

Fig. 7. Variation of mean drag coefficient (C_D) with respect to L/H for various E/H at $\mathrm{Re}_\ell = 2.72 \times 10^5$.

With increase of the distance L/H to 3 and above, the measured pressure distributions for E/H= 0.25 and 0.5 having the stagnation pressure coefficient values of less than unity indicate the disappearance of the deflected gap flow between the bodies (Fig. 6). For $E/H = 1.0$ the mean pressure distributions before and after $L/H = 3$ are similar.

Variation with respect to L/H of the corresponding drag and lift coefficients for different E/H values are determined by the magnitude of the angle the distributions are rotated towards the outside of the wake region of the plate, and the amount of suction produced by a strong shear layer–surface interaction at a small portion of the cylinder surface facing the upstream plate. The variations of drag (C_D) and lift (C_L) coefficients of the downstream cylinder as function of the longitudinal (L/H) and the transverse (E/H) spacings are shown in Figs. 7 and 8, respectively. For $E/H = 0.25$, C_D indicates a variation with L/H, which is similar to that of $E/H = 0$, except that it decreases first, making a minimum at $L/H = 1.5$ and then increases. The variation corresponding to $E/H = 0.5$ does not differ appreciably from the former two for $L/H \geqslant 3$. However, a large deviation from the cases of $E/H = 0$ and 0.25 is observed for smaller longitudinal spacings ($L/H \leqslant 3$). As the cylinder is moved further towards the free-stream ($E/H = 1$), the drag coefficient C_D attains its maximum values for all the longitudinal spacings L/H. Corresponding to the minimum value of C_D for $E/H = 0.25$ at $L/H = 1.5$, the lift coefficient C_L indicates a maximum (Figs. 7 and 8). For increasing E/H, the location of the lift

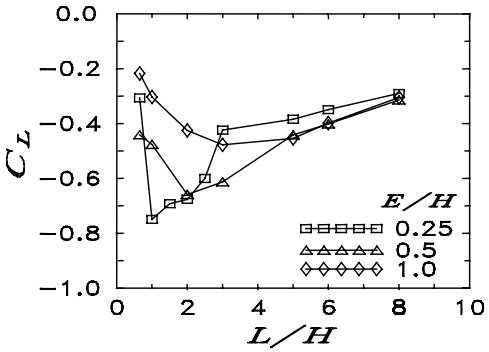

Fig. 8. Variation of mean lift coefficient (C_L) with respect to L/H for various E/H at $\mathrm{Re}_\ell = 2.72 \times 10^5$.

maximum shifts towards larger values of the longitudinal spacing L/H. Additionally, the maximum value of the negative lift decreases with increasing transverse spacing E/H.

4. Concluding remarks

This experimental study reveals existence of a critical spacing L/H which marks the boundary on either side of which different flow interferences take place, not only for the tandem but also for the staggered arrangements of the blunt-based flat plate of thickness H and the circular cylinder of diameter D.

For the tandem arrangement, presumably due to the fact that the boundary layers on the upper and lower surfaces of the plate develop into much thicker separated layers and the cross-stream length scale ratio of $D/H = 0.75$ is larger in comparison with the case of cylinder pair (Igarashi, 1982), the synchronized flow pattern characterized by a large negative drag of the downstream cylinder is completely by-passed, and thus the gap flow remained stagnant for large values of longitudinal spacing extending up to the critical. For $L/H = 2.85$ and higher values of longitudinal spacing, the separated layers from the plate roll up in front of the cylinder.

In the case of the staggered arrangement, about the same critical longitudinal spacing L/H is evidenced in terms of the mean pressure distributions around the base of the upstream plate and those around the downstream cylinder. Whereas the pressure distributions around the base of the plate are not symmetric with respect to the centerline of the plate and are dependent on the transverse spacing E/H for L/H smaller than the critical, they become symmetric and practically independent of E/H once the critical spacing is exceeded. In agreement with that, for L/H less than the critical, the pressure distributions around the cylinder for different E/H indicate pronounced deflection of the incoming flow towards the gap between the plate and the cylinder, and consequently the front stagnation point of the cylinder shifts away from the gap-side and the pressure coefficient there is around unity. For L/H exceeding the critical, both the amount of shift in the stagnation point location and the value of the pressure coefficient at that location decrease.

A numerical analysis of the subject flows, based on vortex methods, will be the subject of a follow-up paper.

Acknowledgements

This study has been supported by NATO under Research Grant No. CRG972960 and the Istanbul Technical University research fund. We would like to thank our reviewers for many useful suggestions in improving the quality of this paper.

References

Breugelmans, F.A.E., Junkhan, G., 1973. Probes for pressure measurements. VKI for Fluid Dynamics, Course Note 82, Rhode Saint Genese, Belgium

Gu, Z.F., Sun, T.F., 1999. On interference between two circular cylinders in staggered arrangement at high subcritical Reynolds number. Journal of Wind Engineering and Industrial Engineering 80, 287–309.

Hiwada, M., Taguchi, T., Mabuchi, I., Kumada, M., 1979. Fluid flow and heat transfer around circular cylinders of different diameters in cross flow. Bulletin of the JSME 22 (167), 715–723.

Igarashi, T., 1981. Characteristics of the flow around two circular cylinders arranged in tandem. Bulletin of the JSME 24 (188), 323–331.

Igarashi, T., 1982. Characteristics of a flow around two circular cylinders of different diameters arranged in tandem. Bulletin of the JSME 25 (201), 349–357.

Keser, H.İ., 1995. Flow around two bluff bodies in tandem and staggered arrangements by the discrete vortex method and experiment. Ph.D. Dissertation, Institute of Science and Technology, Aeronautical Engineering Program, Istanbul Technical University, Istanbul, Turkey.

Okajima, A., 1979. Flows around two tandem circular cylinders at very high Reynolds numbers. Bulletin of the JSME 22 (166), 504–511.

Sumner, D., Price, S.J., Paidoussis, M.P., 2000. Flow-pattern identification for two staggered circular cylinders in cross-flow. Journal of Fluid Mechanics 411, 263–303.

Zdravkovich, M.M., 1977. Review of flow interference between two circular cylinders in various arrangements. ASME Journal of Fluids Engineering 99, 618–631.

Zdravkovich, M.M., 1987. The effects of interference between circular cylinders in cross flow. Journal of Fluids and Structures 1, 239–261.